Improvement of EC-Driven Spherical Tokamak Discharge by a Radial Magnetic Perturbation on Energetic Trapped Electrons

Fumitake WATANABE, Masaki UCHIDA, Hitoshi TANAKA and Takashi MAEKAWA

Graduate School of Energy Science, Kyoto University, Kyoto 606-8502, Japan

(Received 9 November 2011 / Accepted 22 December 2011)

Effects of a radial magnetic perturbation (MP) on electron cyclotron (EC) driven fast electrons are investigated in the Low Aspect ratio Torus Experiment (LATE) device. When a weak MP is applied to plasmas maintained solely by EC heating and current drive, plasma current and electron density increase, whereas energetic trapped electrons located outside the last closed flux surface (LCFS) on the low field side (LFS) decrease. The effect of MPs on energetic trapped electrons has an important role in improving EC-driven plasma discharges.

Keywords: Radial magnetic perturbation, spherical tokamak, electron cyclotron heating, current drive, fast electron, energetic passing electron, energetic trapped electron, LATE

DOI: 10.1585/pfr.7.1202005

Non-inductive plasma current start-up and ramp-up by EC heating and current drive have been developed in recent experiments on the LATE device [1–3]. Although the plasma current is carried mainly by EC-driven energetic passing electrons in these experiments, many energetic trapped electrons exist outside these low aspect ratio plasmas [3]. Understanding the confinement properties of these fast electrons is important for improving the performance of these EC-driven plasmas. In the LATE device, the effects of externally applied radial MPs on both the energetic passing and trapped electrons have been investigated. Previous studies of medium-sized tokamaks [4, 5] with externally applied MP coils investigated the transport of runaway electrons having mainly high-energy passing components. However, the effect of the externally applied MP on energetic trapped electrons is still not clearly understood. Present MP studies on LATE may provide new information.

Figure 1 shows the MP coils in the LATE device, which consist of two coils surrounding the horizontal port sections outside the vacuum vessel. Each coil's winding number is 25 turns, and the maximum current in each coil (I_{MP}) is 2.5 kAT. The coils create a radial MP (δb_r), as shown in Fig. 1, where $+\delta b_r$ corresponds to a radially outward directed MP. The applicable normalized MP strength is $|\delta b_r|/B_t \leq 1.8\times10^{-2}$ at $R = 0.25$ m and $B_t = 480$ G where B_t is the toroidal field at the torus center and R is the major radius. In LATE plasmas, the safety factor at the LCFS (q_{LCFS}) is very high. The achieved q_{LCFS} is approximately 30, which is evaluated for a 20 kA plasma current ramp-up discharge under a magnetic configuration of $B_t = 690$ G and $B_v \sim 190$ G [3] where B_v is the vertical field strength at $R = 0.25$ m. Therefore, the MP spectra of LATE plasmas exhibit mainly non-resonant components.

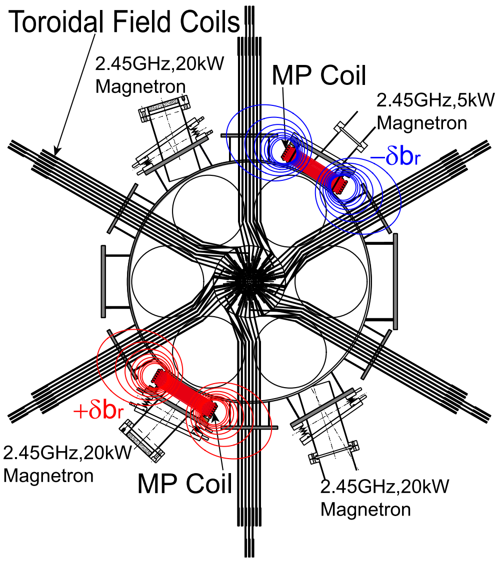

Fig. 1 MP coils and 2.45 GHz magnetron system in the LATE device.

Figure 2 shows a typical waveform when the plasma current (I_p) ramps up as the microwave power (P_{rf}) and B_v are increased and then maintains a flat-top value of $I_p \sim 7$ kA after P_{rf} and B_v are kept constant. When the MP ($|\delta b_r|/B_t \sim 3.6\times10^{-4}$ at $B_t = 480$ G) is applied during this final flat-top phase, I_p increases by 10% (Fig. 2 (c)). At this time, characteristic variations in the loop voltage at $R = 27$ cm (V_L) and vertical current center (Z_j) are not seen (Figs. 2 (d) and 2 (f)), whereas the radial current center (R_j) is shifted slightly to the outside (Fig. 2 (e)). Figure 2 (g) shows the line-integrated electron density (n_eL) along the vertical chord at $R = 27$ cm. The line-averaged electron density ($\bar{n}_e$) estimated from n_eL

author's e-mail: fumitake.watanabe@fx2.ecs.kyoto-u.ac.jp

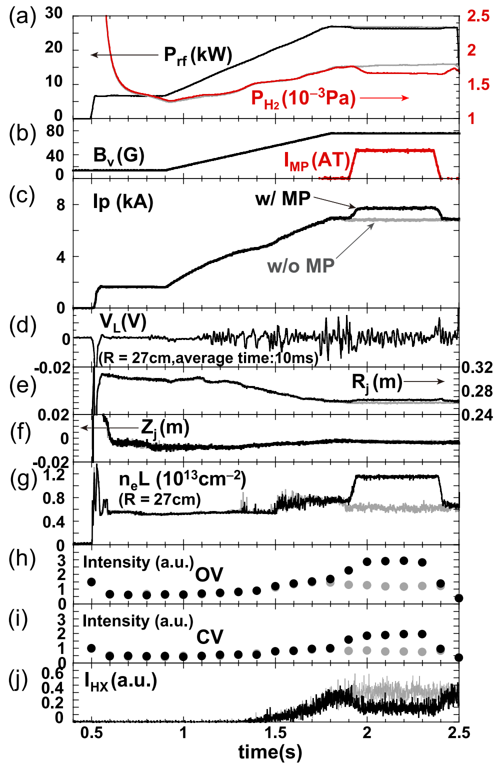

Fig. 2 Time traces of an EC heating and current driven plasma with a steady MP (I_{MP} = 50 AT at t = 1.9–2.4 s) and without the MP (gray line).

increases by roughly 16%, where $\bar{n}_e$ in the non-MP and MP phases (t = 1.86 s and 2.33 s) is ~2.88×10^{11} cm^{-3} (L = 0.26 m) and ~3.33×10^{11} cm^{-3} (L = 0.36 m), respectively. As shown in Figs. 2 (h) and 2 (i), two impurity line radiations of OV and CV with high excitation energies of 72 eV and 304 eV, respectively, are enhanced during MP, suggesting an increase in electron temperature. Figure 2 (j) shows the hard X-ray (HX) emission observed by a NaI scintillator having a line of sight to the center post through the plasma. The HX emission increases rapidly as I_p and B_v increases, suggesting a rapid increase in energetic trapped electrons that hit the center post and emit strong X-rays. Applying the MP strongly suppresses the increased HX emission.

This improvement in EC-driven plasma discharges is observed in the range of $I_p > 5$ kA with $B_v > 50$ G, in which the HX emission is strongly developed. When the flat-top I_p value is below this range, the MP slightly decreases I_p. For flat-top discharges similar to that in Fig. 2, the improvement is obtained in the range $I_{MP} \leq 75$ AT and $|\delta b_r|/B_t \leq 5.4 \times 10^{-4}$, whereas a slightly stronger MP ($I_{MP} \geq 125$ AT and $|\delta b_r|/B_t \geq 9.0 \times 10^{-4}$) induces a decrease in plasma current, which sometimes terminates the discharge.

Figures 3 (a) and 3 (b) show the radial profiles of plasma pressure estimated by an equilibrium analysis based on the anisotropic pressure model by making use

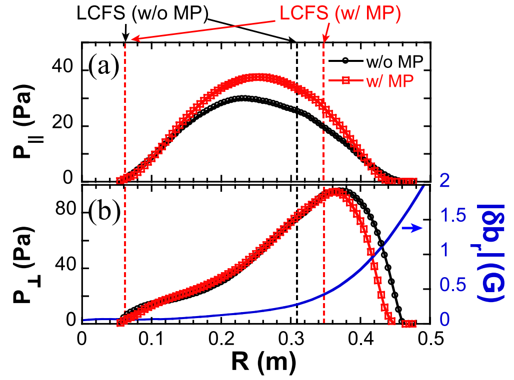

Fig. 3 Radial profiles of (a) parallel and (b) perpendicular pressure with and without the applied MP on a horizontal cross-section of the discharge in Fig. 2 (t = 1.86 s and 2.33 s), and the applied δb_r profile for I_{MP} = 50 AT.

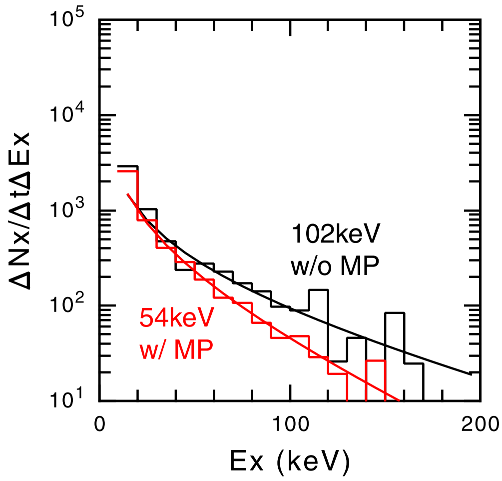

Fig. 4 HX energy spectra with and without the applied MP at R = 0.355 m.

of flux signals [3], where the difference between the flux signals and the fitted data is less than 1%. Here, $P_{\parallel}$ and $P_{\perp}$ indicate the pressures of components parallel and perpendicular to the magnetic field, respectively. Note that the contribution of bulk electrons to the pressure is negligible, and the profiles reflect the fast electron pressure. EC heating generally accelerates electrons primarily in the direction perpendicular to the magnetic field. Therefore, in these EC-driven plasmas, $P_{\perp}$ is fairly large compared with $P_{\parallel}$, and the peak position is located outside the LCFS on the LFS. Applying an MP clearly reduces $P_{\perp}$ outside the LCFS on the LFS but leaves $P_{\parallel}$ unchanged. Furthermore, the increase in $P_{\parallel}$ inside the LCFS amplifies the LCFS on the LFS. Figure 4 shows the HX energy spectra, measured along the vertical chord at R = 0.355 m outside the LCFS. Applying the MP decreases the photon count, especially in the high-energy range. Note that the HX emission originates mainly in energetic trapped electrons located outside the LCFS on the LFS because it has been confirmed that the radial profile of photon counts with energies from 25 to 200 keV is similar to that of $P_\perp$ in a $I_p \sim 13$ kA plasma discharge [6].

The above pressure profile and HX measurements clearly indicate that applying an MP increases the number of passing electrons, whereas the trapped component is decreased. Two possible explanations are suggested. Microwave power from outside is first encountered and absorbed by the energetic trapped electrons, and then the remaining power is absorbed by the energetic passing electrons located inside the LCFS. If the application of an MP could induce a loss in the trapped electrons at their initial low energy level during EC heating, absorption by the trapped electrons decreases, and a larger power reaches the plasma core and heats the passing electrons. Direct conversion from the trapped component to the passing one via enhanced pitch angle diffusion due to the MP might be another possibility.

This work was supported by a Grant-in-Aid for Japan Society for the Promotion of Science Fellows (No. 215858).

[1] T. Maekawa *et al.*, Nucl. Fusion. **45**, 1439 (2005).
[2] T. Yoshinaga *et al.*, Phys. Rev. Lett. **96**, 125005 (2006).
[3] M. Uchida *et al.*, Phys. Rev. Lett. **104**, 065001 (2010).
[4] H. Kawashima *et al.*, J. Plasma Fusion Res. **70**, 868 (1994).
[5] K.H. Finken *et al.*, Nucl. Fusion **47**, 91 (2007).
[6] H. Tanaka *et al.*, Proc. 19th Topical Conf. on Radio Frequency Power in Plasmas (Newport Rhode Island, 2011).